Received: 21 February 2022 | Revised: 7 April 2022 | Accepted: 2 May 2022

DOI: 10.1002/jbio.202200051

RESEARCH ARTICLE

JOURNAL OF BIOPHOTONICS

Depth of focus extension in optical coherence tomography using ultrahigh chromatic dispersion of zinc selenide

Maria N. Romodina[1*] | **Kanwarpal Singh**[1,2]

[1]Max Planck Institute for the Science of Light, Erlangen, Germany

[2]Department of Physics, Friedrich Alexander University Erlangen-Nürnberg, Erlangen, Germany

***Correspondence**
Maria N. Romodina, Research Group Singh, Max Planck, Institute for the Science of Light, Staudtstr. 2, Erlangen 91058, Germany.
Email: maria.romodina@mpl.mpg.de

Funding information
Max-Planck-Gesellschaft

Abstract

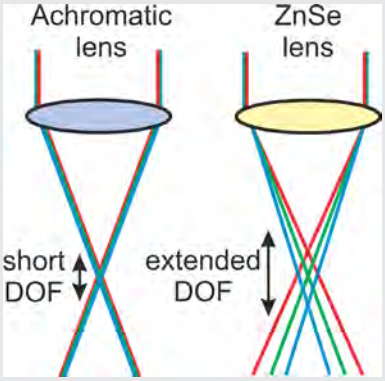

We report a novel technique to overcome the depth-of-focus limitation in optical coherence tomography (OCT) using chromatic dispersion of zinc selenide lens. OCT is an established method of optical imaging, which found numerous biomedical applications. However, the depth scanning range of high-resolution OCT is limited by its depth of focus. Chromatic dispersion of zinc selenide lens allows to get high lateral resolution along extended depth of focus, because the different spectral components are focused at a different position along axes of light propagation. Test measurements with nanoparticle phantom show 2.8 times extension of the depth of focus compare to the system with a standard achromatic lens. The feasibility of biomedical applications was demonstrated by ex vivo imaging of the pig cornea and chicken fat tissue.

KEYWORDS

chromatic dispersion, cornea tissue, depth of focus, fat tissue, imaging, optical coherence tomography

1 | INTRODUCTION

Optical coherence tomography (OCT) is a well-known method of three-dimensional (3D) imaging of biomedical tissues, which has a lot of applications in medical diagnostics [1]. OCT is widely used for clinical applications in ophthalmology [2, 3], cardiology [4], and endoscopy of gastrointestinal tract [5, 6]. The main advantage of this method is high resolution up to micrometer level in combination with a few mm penetration depth [7, 8]. The resolution along light beam propagation (axial resolution) is inversely proportional to the width of the light source spectrum and can be improved by the use of a broadband light source. Lateral resolution is defined by the numerical aperture of the imaging lens, and it decreases significantly moving away from a focal point due to the rapid divergence of light once it is focused to a small spot. There is a

Abbreviations: DOF, depth of focus; OCT, optical coherence tomography; ZnSe, zinc selenide.

trade-off between lateral resolution and the depth of focus (DOF) in OCT with conventional optical elements, and it significantly limits the scope of applications.

To overcome the DOF limitation in OCT with a high lateral resolution, various approaches have been proposed. An axicon lens has been used to produce an effective DOF of 6 mm with a lateral resolution of 10 μm [9], however, the imaged part carried only ~5% of the total power, limiting its application for biomedical samples. Binary-phase spatial filters have been used to optimize the point-spread function of the microscope and extend the DOF up to 10 times with a resolution up to 5 μm [10, 11]. In this approach, the beam has the Bessel intensity distribution and suffers a major loss of spatial frequency components in the coherence transfer function (CTF) compared to the Gaussian beams, thus, the sensitivity decreases and sidelobe artifacts appear in the OCT images. A multiple aperture synthesis technique has been used to achieve DOF extension without signal loss or sidelobe artifacts, however, it requires transversel shifting of micro cylindrical lens near the tip of the sample fiber during the imaging process, and it limits the speed of imaging and makes complicated the endoscopic applications of proposed technique [12]. Adaptive optics approach was used to extend DOF by dynamic control of deformable mirror and introducing spherical aberrations [13]. A few computational algorithms for the automation of interferometric synthetic aperture microscopy and computational adaptive optics were used to significantly extends the depth of field [14], however, algorithmic processing of images is time consuming and can take dozens of minutes. Gabor domain OCT allows to perform dynamic focusing without mechanical motion of optical elements by adjusting the voltage applied to the liquid lens [15].

The idea to use the optical elements with chromatic dispersion to achieve high transverse resolution over an extended DOF has been explored before. Chromatic dual-focus fiber-optic probe has been used to extend DOF by two times compared to common single focus probe [16]. Also, recently the metalens with chromatic dispersion was used to maintain high-resolution endoscopic imaging beyond the input field Rayleigh range [17]. In these approaches, complicated design solutions are used to introduce chromatic dispersion to a system. To use an imaging lens, made from material with low Abbe number and high chromatic dispersion seems to be a simpler, but promising idea.

Here, we demonstrate high-resolution volumetric OCT imaging with extended DOF due to high chromatic dispersion of zinc selenide (ZnSe) lens [18]. ZnSe has a strong spectral dispersion for light in the visible and near-infrared region [18]. Different components from the source with a wide spectrum are focused at a different positions along the beam axis using the ZnSe lens. Ex vivo imaging of the pig cornea and chicken fat tissue demonstrates the ability to obtain images with subcellular resolution, which can extend the utility of OCT in clinical diagnostic and monitoring of diseases.

2 | EXPERIMENTAL SECTION

The schematic of the experimental setup is shown in Figure 1. We used a swept-source OCT system (Axsun Technologies, North Billerica, Massachusetts). The central wavelength equals 1310 nm with a scan range of 140 nm at a sweeping rate of 100 kHz. The output power of the source is 24 mW. Additional to the illumination unit, the system comes with components for data acquisition and processing. Two photodiodes enabling balanced detection are coupled to a data acquisition card, a digitizer and a field-programmable gate array. To realize OCT with extended depth of focus, we build a free-space module. The light of the source was divided into two parts using a beam splitter (BS1), 10% of light went to the reference arm and 90% of light went to the sample arm. The light in the reference arm was collimated, reflected by the reference mirror and coupled back to the fiber. The light in the sample arm was illuminated from the fiber tip and filled the full aperture of the ZnSe lens (39 495, Edmund Optics) with the focal distance $f = 50.8$ mm. Then, the beam was deflected by a galvo-mirror, allowing scanning of the sample along the x-axis. Scanning along the y-axis was performed using a piezo stage (AG-LS25-27, Newport Corporation). The numerical aperture of the beam focused on the sample was equal to 0.14, giving the best lateral resolution about 4.7 μm. The light reflected from the sample was collected and coupled back to fiber. The beams reflected from the sample and the reference arms were guided by optical circulators and combined using beamsplitter (BS2). Polarization controllers PC1 and PC2 were adjusted to balance the reference power on the balanced photodiodes D1 and D2. The interference pattern was measured using the balanced photodiodes D1 and D2 incorporated in the OCT engine.

To compare the performance of the developed system with the conventional approach, we made the measurements with the same system, but with an achromatic lens instead of the ZnSe lens. The light coming from the fiber in the sample arm was collimated to a beam with a diameter of 12 mm. Then, it was incident on achromatic doublet (AC254-030-C-ML, Thorlabs, 30 mm focal lens), which was selected to have the same numerical aperture of the focused beam to provide the same lateral resolution as the system with the ZnSe lens.The idea of the

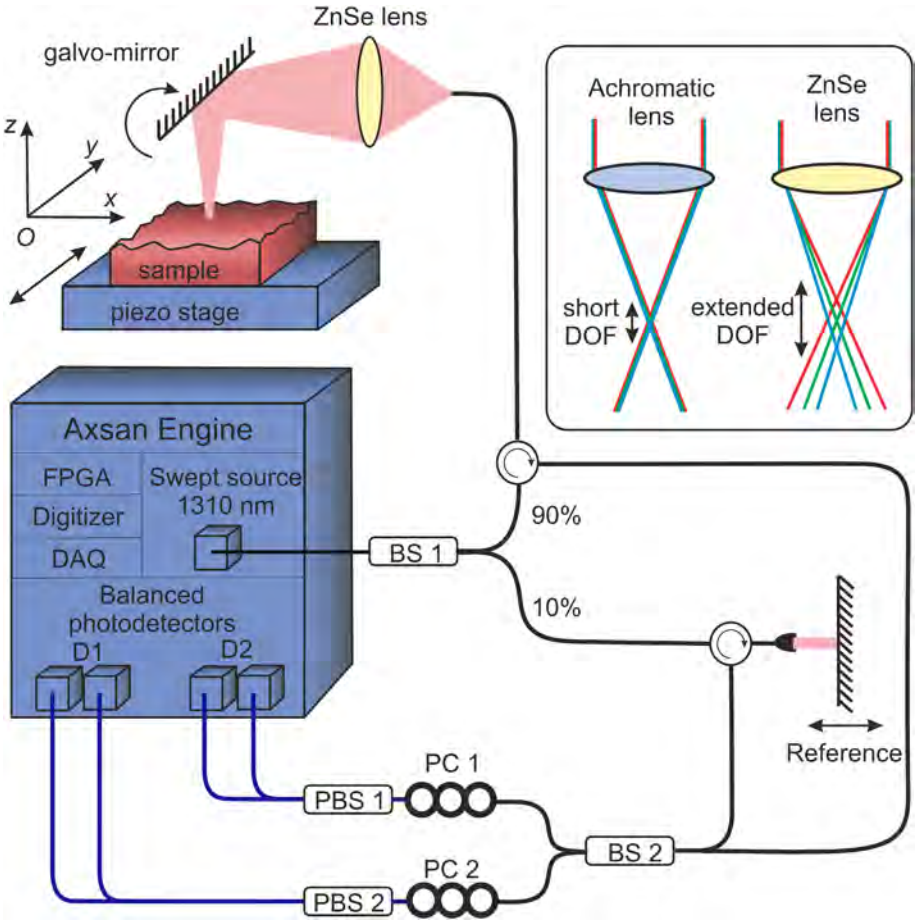

FIGURE 1 Schematic of the experimental setup of optical coherence tomography (OCT) with ZnSe lens. BS1 and BS2 are beam splitters, PBS1 and PBS2 are polarized beam splitters, PC1 and PC2 are polarization controllers. The inset: a schematic of the depth of focus extension using chromatic dispersion of ZnSe lens]

depth of focus extension using ZnSe lens is schematically illustrated in the inset of Figure 1. For the achromatic lens, all spectral components are focused at one position and transversal resolution dramatically decreases moving away from the focal point along beam propagation due to rapid divergence of the beam. Using the ZnSe lens, the different wavelengths are focused at different positions along the beam propagation axis, and for every position inside extended depth of focus, there are some spectral components that are tightly focused and give the image with high lateral resolution.

3 | RESULTS

3.1 | Numerical simulations

Numerical calculations of the depth of focus extension with ZnSe lens were made in Zemax software. The results of the numerical calculation are shown in Figure 2. Light coming out from the fiber illuminates the whole aperture of the ZnSe lens and is focused at a distance of about 87 mm away from the lens. Numerically calculated ray diagram for the light with wavelength of 1310 nm (the central wavelength of the spectra), which propagates from the fiber end and is focused by ZnSe lens is shown in Figure 2A. Different wavelengths of spectra are focused at different positions away from the lens because of the chromatic dispersion of lens material. The depth of focus can be estimated as a difference between focal points for light components with $\lambda = 1.24$ μm and $\lambda = 1.38$ μm and approximately equals to 650 μm. The lateral distributions of the relative irradiance at the focal points are shown in Figure 2B. The light is focused to spots, with half of the maximum widths of 5 μm for central ($\lambda = 1.31$ μm) and extreme ($\lambda = 1.24$ μm and $\lambda = 1.38$ μm) wavelengths. It is expected that system will have a resolution of about 5 μm along 650 μm focal depth for imaging in the air.

3.2 | Resolution test

To estimate the performance of the developed system, the resolution tests were performed. As the first test object, we imaged a 1951 USAF Resolution Test Target (R3L3S1N, Thorlabs Inc.). The images obtained using systems with ZnSe lens and achromatic lens are shown

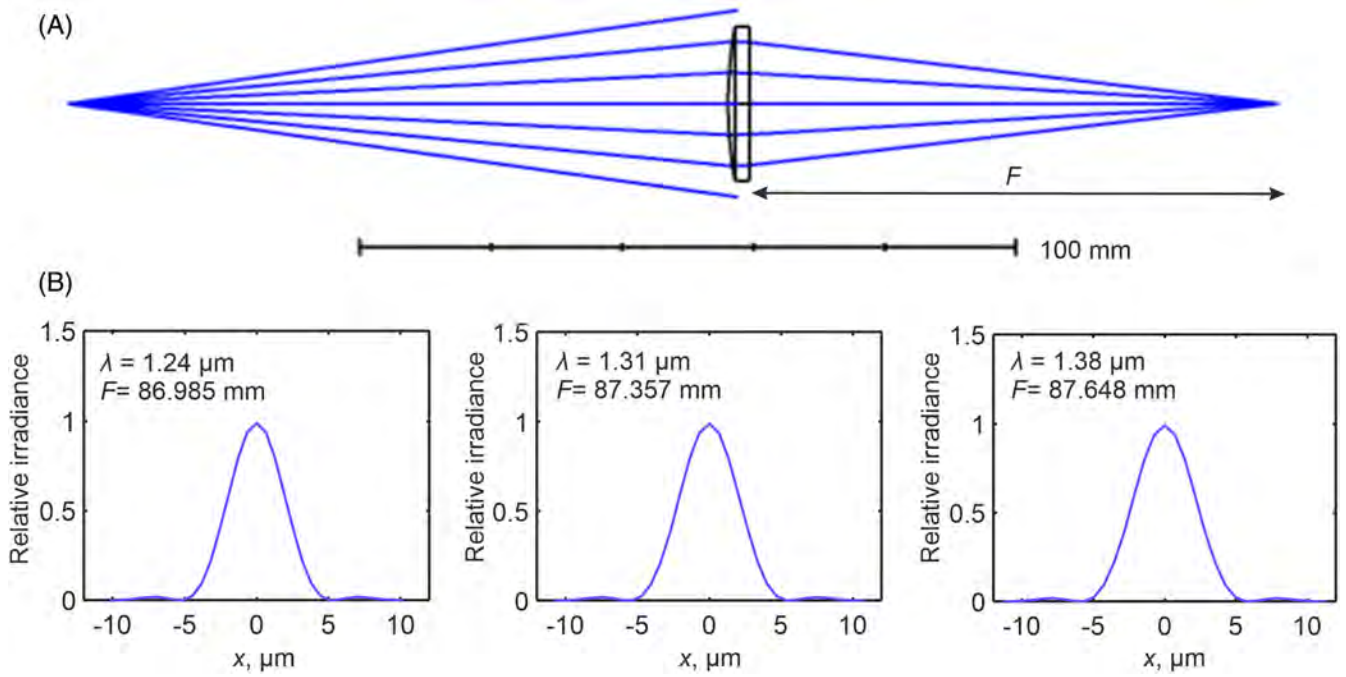

FIGURE 2 The results of numerical simulations made in Zemax. (A) Ray diagram of the light propagation from fiber end and focusing by ZnSe lens. (B) Numerically calculated relative irradiance distribution along focal plane for three different wavelengths in the spectrum. Different wavelengths are focused at different points away from the lens, the distance from the lens to a focal point *F* is provided in the caption of graphs

in Figure 3B. Both systems when focused can resolve element 6 of group 6 (114 lines pairs per mm [lp/mm]) which corresponds to a resolution of 4.4 μm. The system with ZnSe lens is able to maintain this resolution even 200 μm away from the focal point. The quality of images acquired with the achromatic lens at 200 μm away from the focal point is significantly lower, and only the stripes in group 6, element 2 (71.8 lp/mm) can be resolved, showing 1.6 times decrease in resolution.

The second test object was a phantom with nanoparticles incorporated in bulk glass material. En face images of particles acquired using systems with ZnSe and achromatic lenses at different locations along the depth are shown in Figure 3A. Nanoparticles are clearly visible at the focal point using both systems. The minimal size of the image of the particle was about 6 μm for both systems, corresponding to the best lateral resolution of systems in the glass media. Actual size of the particles in the phantom is much smaller, so the size of the particle image corresponds to the resolution of the system. In the images acquired with the ZnSe lens, the nanoparticles, which are shown as white dots, are clearly detected at a longer depth. Figure 3C shows the analysis of the images of the nanoparticles in Figure 3A. The lateral resolution of systems was defined as the size of the nanoparticles' images. The lateral resolution as a function of the axial depth is shown in Figure 3C for both systems. At the focal point, both systems have the same resolution about 6 μm. Maximal resolution is lower than in the case of resolution target imaging, because of the light refraction at the air-glass interface, which influences the focusing of the beam. The resolution of the ZnSe system maintains below 8.5 μm (the level is marked with red line and equals to the $\sqrt{2}\omega$, where ω is the minimum spot size at the focal point) along 680 μm in depth, while the conventional achromatic lens-based system gives the same resolution only along 240 μm in axial depth. Thus, we can state that the proposed new technique gives 2.8 times extended DOF. Also, we did the test measurements of axial resolution for both systems using a mirror as a sample. The axial resolution was measured to be 7.5 μm for the system with the ZnSe lens and 5 μm for the system with the achromatic lens. For the system with the ZnSe lens, the axial resolution is lower, because for every plane along scanning depth, only a part of the spectrum will contribute to the imaging. Using Zemax, we calculated the coupled bandwidth reflected from a mirror as a sample and found it to be approximately 80 nm which provides a theoretical axial resolution of 9.5 μm. This value is very close to the axial resolution achieved experimentally with our system.

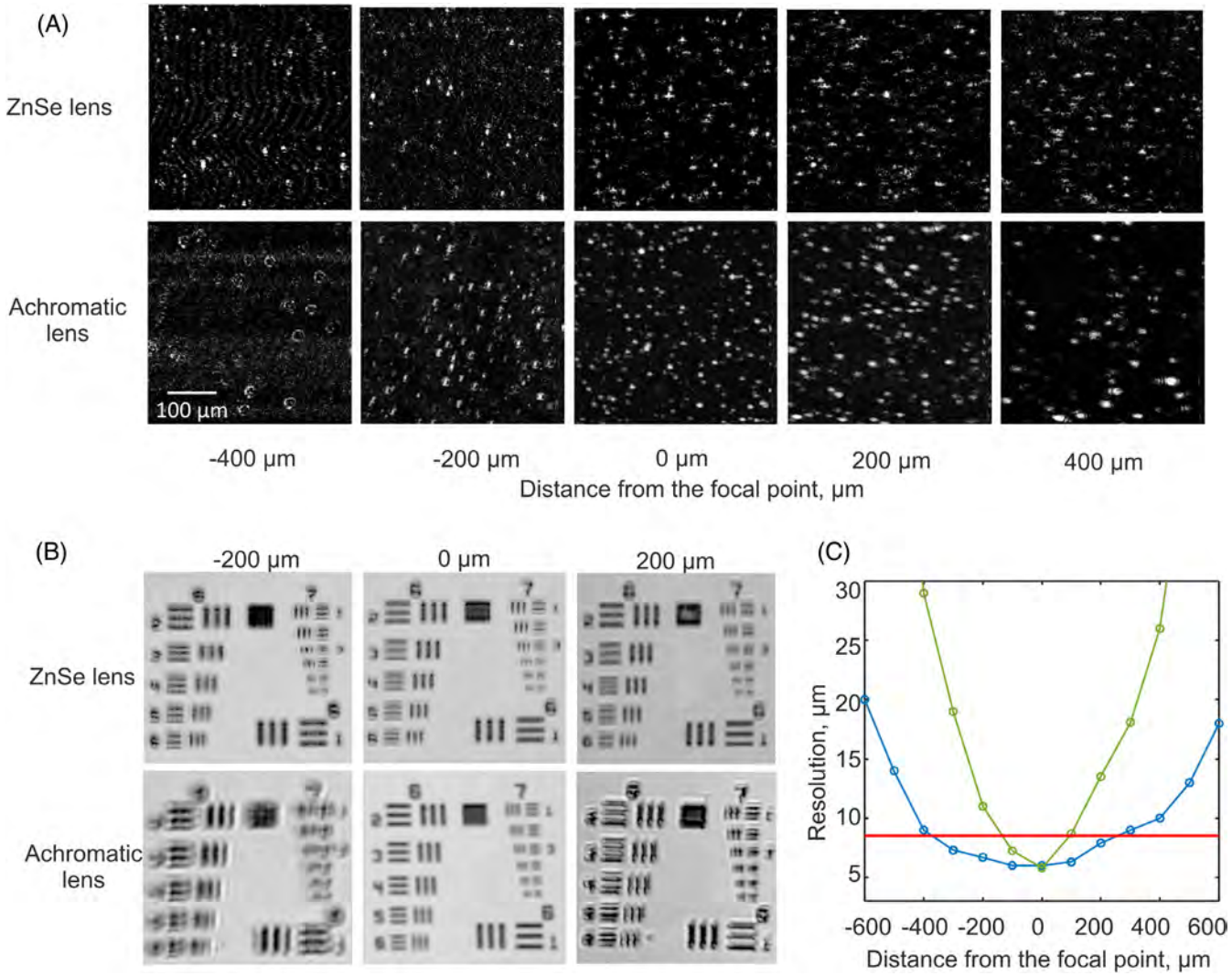

FIGURE 3 (A) The images of nanoparticles phantom made using optical coherence tomography (OCT) systems with ZnSe and achromatic doublet. (B) The images of resolution target obtained using OCT systems with ZnSe lens and achromatic doublet made at different target position relative to the focal point. (C) The resolution for OCT systems with ZnSe lens and achromatic doublet as a function of distance from focal point measured using nanoparticles resolution test

3.3 | Imaging of cornea and chicken fat tissue

To show the feasibility of biological sample imaging with an extended DOF, we carried out ex vivo imaging of a pig cornea and chicken fat tissue. The results of pig cornea images acquired with the achromatic lens system and the system with the ZnSe lens are demonstrated in Figure 4A. In the images acquired with the achromatic lens system, one can see the bright stripe in the middle of the cornea, associated with the imaging focal spot. In contrast, the system with the ZnSe lens provides a uniformly bright image of the cornea due to extended DOF. The chicken fat images acquired with the achromatic lens system and the system with the ZnSe lens are demonstrated in Figure 4B. Both systems clearly demonstrate structural features attributed to the fat cells at the top layer of the sample. However, at the bottom of the sample approximately 800 µm away from the top surface, it is not possible to resolve cells using the achromatic OCT system, while ZnSe lens-based system with extended DOF provides an image with cellular resolution along the whole sample.

4 | DISCUSSION

The results of the imaging of nanoparticles phantom, pig cornea and chicken fat tissue indicate that the effective focal range is extended by a factor of 2.8 due to using ZnSe lens. This extension is higher than the previously proposed chromatic dispersion-based technique [16]. Although binary phase masks and axicon lenses provide much longer

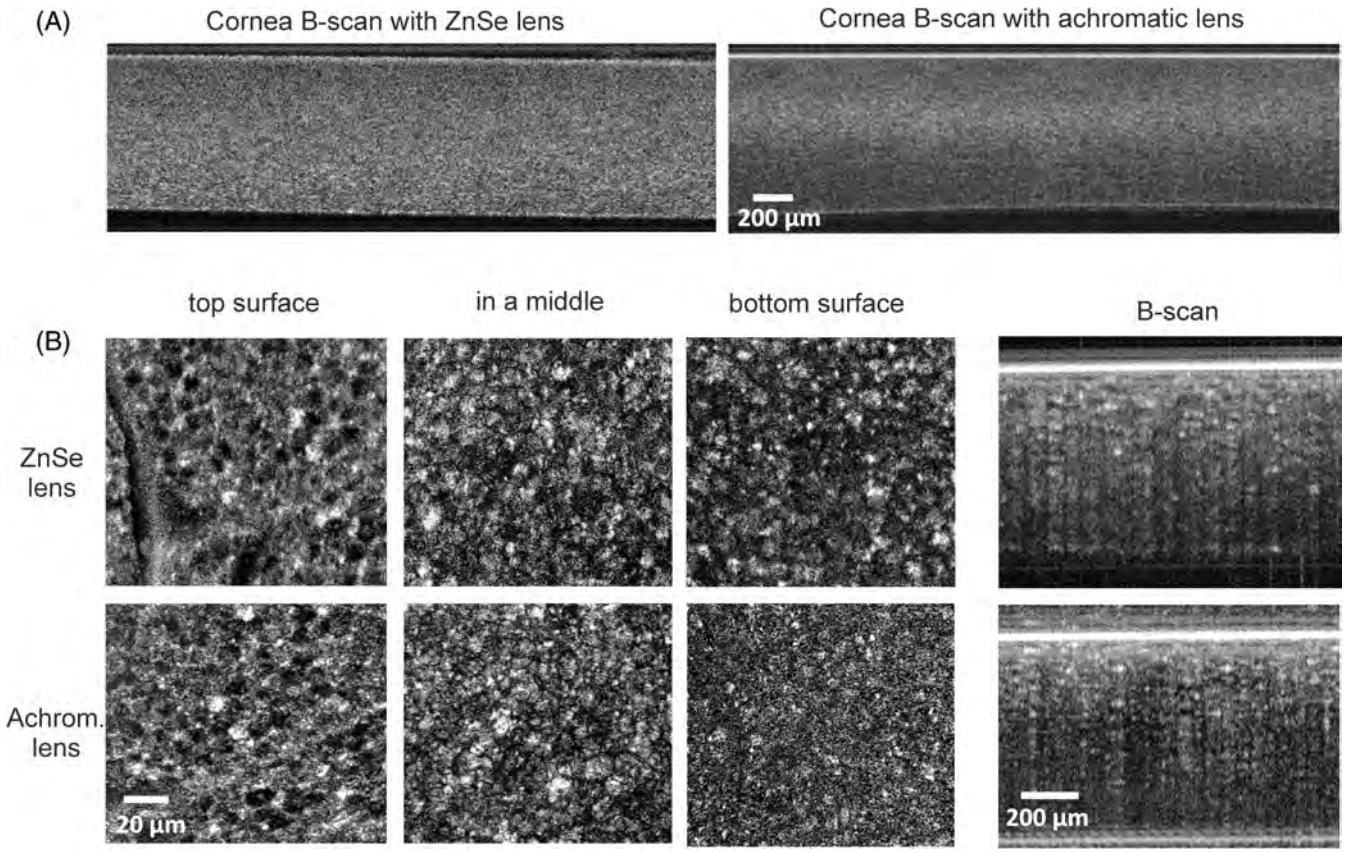

FIGURE 4 The results of ex vivo imaging of biological tissue. (A) Pig cornea cross-sectional images made using systems with ZnSe and achromatic lenses. (B) En face and cross-sectional (B-scan) images of chicken fat tissues. The system with the ZnSe lens demonstrates the cellular features along the whole sample with 800 µm depth

extension DOF [9–11], the main advantage of the technique proposed here is simplicity. Intrinsic chromatic dispersion of ZnSe material is used to extend the focus, and thus no phase mask, moving prisms or additional lenses are needed to create the chromatic focal shift. Also, no additional time is required for data processing and it makes the proposed technique more attractive compared to computational algorithms and adaptive optics-based techniques [13, 14]. The Gabor domain OCT shows a much longer DOF extension compared to the ZnSe-based OCT, however, it comes with the price: it requires a complicated electronic device to control the focal position of a liquid crystal lens [15]. In our system, we use only one stationary commercially available lens to extend DOF for the imaging and we believe that it makes the system attractive for both commercial and biological applications.

Despite all the listed advantages, the method has also some limitations. First of all, ZnSe is a hazardous material and to use the system for biomedical applications one should prevent the direct contact of lens with the studied living objects and take care while handling these lenses. Second, ZnSe material has lower transmission in the near-infrared region compared to the standard lenses made from fused silica or quartz. ZnSe lens, used in the current study, has 72% transmission for the 1310 nm. Also, only a part of the spectrum is coupled back to the system. The limited transmission and reduced bandwidth lead to a loss in sensitivity. The sensitivity of the system is reduced by approximately 6 dB. Furthermore, the ZnSe lens used in our system is not telecentric and if such a lens is used after the galvo scanner, a typical configuration used in several OCT systems, it would produce a curved imaging field. Commercial telecentric ZnSe lenses are not available yet, but in the future, such lenses can be designed for flat field imaging. Nevertheless, all these limitations are minor and do not cancel the benefits of the proposed technique.

5 | CONCLUSION

We have established a technique to overcome the DOF limitation in high-resolution OCT using chromatic dispersion of a single ZnSe imaging lens. However, since only a part of the whole spectrum contributes to the axial scan at a certain depth, this reduces the axial resolution of the system. In future, this can be mitigated using a smaller focal length lens and larger bandwidth light source.

Nevertheless, the proposed method can provide diffraction-limited lateral resolution over 2.8 times extended DOF. The extension of the focal range was numerically and experimentally confirmed. The new technique allows to get relatively high DOF extension and is technically simpler than previously demonstrated multifocal designs. The results of the ex vivo cornea and fat animal tissue imaging demonstrate the feasibility of the proposed method in clinical and pre-clinical applications.

AUTHOR CONTRIBUTIONS

Maria Romodina and Kanwarpal Singh designed the study. Maria Romodina acquired the data during the study. Maria Romodina wrote the manuscript with key input from all other co-authors. Kanwarpal Singh is the principal investigator for the study.

ACKNOWLEDGMENT

Open Access funding enabled and organized by Projekt DEAL.

CONFLICT OF INTEREST

The authors declare no conflict of interest.

DATA AVAILABILITY STATEMENT

The data that support the findings of this study are available from the corresponding author upon reasonable request.

ORCID

Maria N. Romodina https://orcid.org/0000-0001-5395-368X
Kanwarpal Singh https://orcid.org/0000-0002-6884-8089

REFERENCES

[1] D. Huang, E. A. Swanson, C. P. Lin, J. S. Schuman, W. G. Stinson, W. Chang, M. R. Hee, T. Flotte, K. Gregory, C. A. Puliafito, et al., *Science* **1991**, *254*, 1178.
[2] L. M. Sakata, J. DeLeon-Ortega, V. Sakata, C. A. Girkin, *Clin. Experiment. Ophthalmol* **2009**, *37*, 90.
[3] K. Singh, C. Dion, M. Wajszilber, T. Ozaki, M. R. Lesk, S. Costantino, *Invest. Ophthalmol. Vis. Sci.* **2011**, *52*, 8927.
[4] S. D. Giattina, B. K. Courtney, P. R. Herz, M. Harman, S. Shortkroff, D. L. Stamper, B. Liu, J. G. Fujimoto, M. E. Brezinski, *Int. J. Cardiol.* **2006**, *107*, 400.
[5] T. Tsung-Han, L. L. Cadman, J. T. Arvind, S. Amrita, S. Anne-Fré, J. Virendra, J. B. Jacques, M. Hiroshi, S. N. Norman, N. Eman, *J. Biomed. Opt.* **2017**, *22*, 1.
[6] J. Dong, C. Grant, B. Vuong, N. Nishioka, A. H. Gao, M. Beatty, G. Baldwin, A. Baillargeon, A. Bablouzian, P. Grahmann, *Clin. Gastroenterol. Hepatol.* **2021**, *20*, 756.
[7] K. Singh, G. Sharma, G. J. Tearney, *J. Opt.* **2018**, *20*, 025301.
[8] Y. Wang, Y. Zhao, J. Nelson, Z. Chen, R. S. Windeler, *Opt. Lett.* **2003**, *28*, 182.
[9] Z. Ding, H. Ren, Y. Zhao, J. S. Nelson, Z. Chen, *Opt. Lett.* **2002**, *27*, 243.
[10] L. Liu, C. Liu, W. C. Howe, C. Sheppard, N. Chen, *Opt. Lett.* **2007**, *32*, 2375.
[11] J. Kim, J. Xing, H. S. Nam, J. W. Song, J. W. Kim, H. Yoo, *Opt. Lett.* **2017**, *42*, 379.
[12] E. Bo, Y. Luo, S. Chen, X. Liu, N. Wang, X. Ge, X. Wang, S. Chen, S. Chen, J. Li, *Optica* **2017**, *4*, 701.
[13] K. Sasaki, K. Kurokawa, S. Makita, Y. Yasuno, *Biomed Opt. Express* **2012**, *3*, 2353.
[14] Y. Xu, Y. Z. Liu, S. A. Boppart, P. S. Carney, *Appl Optics* **2016**, *55*, 2034.
[15] C. Canavesi, J. P. Rolland, *Appl Sci-Basel* **2019**, *9*, 2565.
[16] J. Li, Y. Luo, X. Wang, N. Wang, E. Bo, S. Chen, S. Chen, S. Chen, M.-T. Tsai, L. Liu, *Appl. Optics* **2018**, *57*, 6040.
[17] H. Pahlevaninezhad, M. Khorasaninejad, Y.-W. Huang, Z. Shi, L. P. Hariri, D. C. Adams, V. Ding, A. Zhu, C.-W. Qiu, F. Capasso, *Nat. Photon* **2018**, *12*, 540.
[18] G. Sharma, K. Singh, *arXiv* arXiv:2201.12373 **2022**.

How to cite this article: M. N. Romodina, K. Singh, *J. Biophotonics* **2022**, *15*(8), e202200051. https://doi.org/10.1002/jbio.202200051